

How Constrained is the cMSSM?

Diptimoy Ghosh ^{a,1}, Monoranjan Guchait ^{b,2}, Sreerup Raychaudhuri ^{a,3} and Dipan Sengupta ^{b,4}

^{a)} Department of Theoretical Physics, Tata Institute of Fundamental Research,
1, Homi Bhabha Road, Mumbai 400 005, India.

^{b)} Department of High Energy Physics, Tata Institute of Fundamental Research,
1, Homi Bhabha Road, Mumbai 400 005, India.

ABSTRACT

We study the allowed parameter space of the constrained minimal supersymmetric Standard Model (cMSSM) in the light of direct searches, constraints from B -physics (including the recent measurement of the branching ratio for $B_s \rightarrow \mu^+ \mu^-$) and the dark matter relic density. For low or moderate values of $\tan \beta$, the strongest constraints are those imposed by direct searches, and therefore, large areas of the parameter space are still allowed. In the large $\tan \beta$ limit, however, the B -physics constraints are more restrictive, effectively forcing the squark and gluino masses to lie close to or above a TeV. A light Higgs boson could dramatically change the allowed parameter space, but we need to know its mass precisely for this to be effective. We emphasize that it is still too early to write off the cMSSM, even in the large $\tan \beta$ limit. Finally we explore strategies to extend the LHC search for cMSSM signals beyond the present reach of the ATLAS and CMS Collaborations.

PACS numbers: 12.60.Jv, 14.40.Nd, 13.85.Rm

March 3, 2013

¹diptimoyghosh@theory.tifr.res.in

²guchait@tifr.res.in

³sreerup@theory.tifr.res.in

⁴dipan@tifr.res.in

1 Introduction

The early results pouring in from the CERN Large Hadron Collider (LHC) and the remarkable speed and efficiency with which they are being analysed for their physics potential represents a major triumph for the smooth operation of the machine and for the meticulous planning that has gone into every facet of the programme. Even though the LHC has utilised but a small fraction of its energy and luminosity potential, LHC data have already overtaken the LEP and Tevatron results in many search channels. More significantly, apart from some excitement about a possible 125 GeV Higgs boson [1, 2], it is clear from the LHC results presented during the past year or so that there is no new physics ‘around the corner’, and we may have to settle for a long and suspenseful wait before the experiment achieves its first breakthrough in this regard. However, this is no reason for despair, for the LHC still has a long way to go before any serious verdict can be pronounced on the different new physics options currently under consideration.

In this article, we discuss the impact of the latest experimental data on the ‘constrained’ minimal supersymmetric Standard Model (cMSSM) [3]. Some time ago, the cMSSM was often dubbed as the ‘standard model’ of physics beyond the Standard Model (SM), but perhaps because of the string of negative results obtained so far, there has lately arisen a tendency to disparage the cMSSM as a model which makes too many arbitrary assumptions and hence is — not-surprisingly — on the verge of getting ruled out by the LHC data [4, 5]. Such views, are however, less than fair to the cMSSM, for, in many ways, the cMSSM may be regarded as the most simple and economical model of supersymmetry, and the one which would most obviously suggest itself in the absence of contradictory experimental evidence. In fact, if one thinks about it, we should rather regard the multifarious alternatives to the cMSSM which appear in the literature as the ones where extra assumptions are introduced. Moreover, the mere fact that the cMSSM parameter space is getting reduced by experimental searches should not be regarded as a setback for the model, for, after all, Nature corresponds to but a single point in the parameter space. The example of the top quark (and maybe the Higgs boson) serves to clearly illustrate this kind of shrinkage of the parameter space to the actual value.

The purpose of this article is not, however, to pontificate in defence of the cMSSM, but rather to investigate the status of different experimental constraints on this model. Among others, we take up the recent measurement of the process $B_s \rightarrow \mu^+ \mu^-$ by the LHCb Collaboration [6] and study its impact on the cMSSM parameter space in conjunction with other low energy constraints. Since the precision of this particular measurement has increased considerably, one would expect it to rule out a wide swath of the parameter space. We quantify this expectation and find, that while the last statement is certainly true at large values of $\tan \beta$, the constraint weakens and disappears as $\tan \beta$ is lowered. We shall demonstrate that even in the large $\tan \beta$ region, the cMSSM is still a possible explanation of not just the hierarchy problem, but also of the dark matter problem. Finally we shall use a novel strategy using event-shape variables, developed by two of the authors [7], to extend the experimental search for the cMSSM to a region of parameter space which is allowed by all the present constraints, but inaccessible to conventional searches.

The plan of this article is as follows. In the next section we briefly discuss the cMSSM and then go on

to discuss how this is constrained. This is followed by a section in which we map the allowed parameter space by including all the relevant constraints, and thus, focus on the viability or otherwise of the model. Some comments on the impact of a 125 GeV Higgs boson are also included in this section. We then go on to describe our novel search strategy, which enables us to extend the search for cMSSM particles into new regions of the parameter space. A critical summary of our work forms the concluding section.

2 The Model and its Constraints

The cMSSM, whose roots go back to the 1980's, now forms the material of textbooks [3,8], and hence, our description of the model will touch only upon its salient features. The particle content of this model may be summarised as a two-Higgs doublet extension of the SM plus superpartners, for all the particles therein. These will have interactions determined by the SM interactions, except for the soft SUSY-breaking sector, which consists of a set of terms included in an ad hoc manner, with the only constraint that they should not lead to quadratic divergences in the mass of the lightest Higgs boson.

It is postulated that there exists a hidden sector of fields which do not interact with the known SM fields through the known SM interactions. In this hidden sector, SUSY is broken spontaneously, at the cost of having massless goldstinos, which are, however, invisible, being in the hidden sector¹. However, the two sectors can interact through gravity, which is universal, and thus if we integrate out the hidden sector fields from the gravity-mediated interactions terms we are left with effective interactions which are just the soft SUSY-breaking terms. This will take place at some high energy scale below the Planck scale. At this scale, all the soft SUSY-breaking terms are generated purely by gravitational interactions, which are blind to all the SM quantum numbers, such as colour, flavour, etc. and sensitive only to space-time quantum numbers such as energy, momentum and spin. Accordingly, at this scale, we must assume that there is a common scalar mass m_0 , a common fermion mass $m_{1/2}$ and a common trilinear coupling A_0 in addition to the Higgsino-mixing parameter μ . Any splitting among these (known as *non-universality*) would require the hidden sector to be sensitive to the global SM quantum numbers (e.g. flavour) which distinguish the different visible fields. We do not make this assumption in the cMSSM, partly in the interests of economy, but also because it is hard to conceive of the hidden sector fields as carrying the global, but not the local, quantum numbers of the SM sector.

Once we have generated the soft SUSY-breaking terms at a high scale, we have a theory where sparticle masses of a given spin are universal. It is usual to identify this scale with the scale for grand unification (GUT scale). The mass spectrum of the model at the electroweak scale is now generated by allowing the masses and couplings to run down from the GUT to the electroweak scale using the renormalisation group equations (RGE) for the model. Some judicious manipulation of independent parameters replaces the free parameter μ by its sign, and the ratio of vacuum expectation values (VEVs) of the two Higgs boson doublets (at the electroweak scale), which is denoted by $\tan\beta$. This is a natural parametrisation that ensures that one of the Higgs mass parameters is driven negative at precisely the electroweak scale – which provides an ‘explanation’ of the phenomenon of electroweak symmetry-breaking (EWSB).

¹In supergravity models, this goldstino is absorbed into the massive gravitino.

Thus the cMSSM has several merits. It does not require much input from the hidden sector except supersymmetry-breaking, but we can generate the entire spectrum of masses, couplings and mixing angles in terms of just four parameters and a sign, viz. m_0 , $m_{1/2}$, A_0 , $\tan\beta$ and the sign of μ . All that one has to do then, is to choose a point in this limited parameter space, and the entire gamut of SUSY phenomenology is uniquely determined by this choice. For this reason, and for the theoretical niceties described above, the cMSSM has been the favourite choice for studies of new physics beyond the SM.

In recent times, we have seen a breaking-away from the cMSSM paradigm, with the introduction of several non-universal versions of SUSY [9]. Though these offer a richer phenomenological fare — which is to be expected when the number of free parameters increases — all these models have, implicitly or otherwise, to make some assumptions about the hidden sector which the cMSSM does not. This is not to say that non-universal models should not be investigated, but it should be clear that from the point of view of economics and aesthetics, that the cMSSM has definite advantages.

Given the above, it is not surprising that the cMSSM is often given top priority whenever experimental searches for new physics beyond the SM are considered. This is indeed so, and has been the case for the past few decades. Of course, all such searches till date have yielded negative results and only succeeded in ruling out parts of the cMSSM parameter space. It is important, therefore, to see how these restrictions arise, and how seriously one should take them. Constraints on the cMSSM arise from four main sources. These are listed below.

- *Theoretical Considerations:* Except for rather loose naturalness considerations, there are no *a priori* theoretical guidelines for the choice at the GUT scale of values of m_0 , $m_{1/2}$ and A_0 , or the sign of μ . For $\tan\beta$, however, we note that the Yukawa couplings of the top and bottom quarks remain comfortably perturbative so long as $1.2 \lesssim \tan\beta \lesssim 65$ [8].

Very small values of m_0 and $m_{1/2}$ (\sim few GeV) are not viable in the cMSSM, for then the RGE would drive the electroweak symmetry-breaking to happen rather close to the GUT scale, and this would imply a much lower GUT scale than appears to be indicated by the measured running of the gauge coupling constants. For larger values of m_0 and $m_{1/2}$, there arise two kinds of *a posteriori* constraints which act collectively on the parameters m_0 , $m_{1/2}$ and A_0 when the cMSSM spectrum is run down from the GUT scale to the electroweak scale. One is the requirement that the scalar potential in the theory remain bounded from below – this is referred to as the *vacuum stability* constraint [10]. The other is the requirement that the lightest SUSY particle (LSP) be a neutral particle – which is demanded if it is to be the major component of dark matter. This is found to rule out a region of the parameter space where the RGE evolution makes the lighter stau $\tilde{\tau}_1$ the LSP.

Another consideration, which is not a constraint but may be regarded as some sort of wishful thinking, is a requirement that the parameters m_0 , $m_{1/2}$ and A_0 not be much more than a few TeV. This is because higher values of these parameters – especially the first two – tend to drive the masses of all the SUSY particles outside the kinematic range of the LHC (and even its foreseeable successors), while the lightest Higgs boson mass gets pushed close to a value around 120 GeV. In this, so-called *decoupling limit* the cMSSM Higgs boson would be indistinguishable, for all practical purposes, from its SM counterpart. Such a scenario, though by no means impossible,

would be a great disappointment for seekers of new physics, as it would leave the existence of SUSY as a wide open question without a hope of solution in the near future. Of course, requiring the m_0 , $m_{1/2}$ and A_0 to be in this convenient range is essentially dogma, but it is what renders studies of the present kind worth carrying out.

- *Indirect effects at low-energy experiments:* The cMSSM can affect low-energy processes when the relatively-heavy superparticles appear in Feynman diagrams at the loop level. Any measurement of a low-energy process which (a) get contributions from these particles, and (b) is measured with sufficient accuracy to access these usually small effects, will impose a constraint on the cMSSM. Based on these two criteria, we can now discern *three* distinct types of low-energy constraints.

1. The first type is where the low-energy effect is observed and measurement is consistent with the SM prediction. In this case, any contributions from the cMSSM will have to be small enough to fit into the small leeway allowed by the error bars. Such constraints have a tendency to get tighter and tighter as more data are collected in an experiment and the error bars shrink. The relevant example of this is the radiative B decay $B \rightarrow X_s \gamma$, where the measured value of the branching ratio $\text{BR}(B \rightarrow X_s \gamma)$ is $(3.55 \pm 0.24 \pm 0.09) \times 10^{-4}$ [11] against an SM prediction of $(3.15 \pm 0.23) \times 10^{-4}$ [12]. Thus, including the intrinsic cMSSM uncertainty of about 0.15×10^{-4} as given in [13] (which was based on [14], we can set the 95% allowed range to be $(3.55 \pm 0.95) \times 10^{-4}$. This means that the cMSSM contribution must satisfy

$$-0.55 \times 10^{-4} \leq \text{BR}_{\text{cMSSM}}(B \rightarrow X_s \gamma) \leq 1.35 \times 10^{-4} .$$

2. The second type is where the SM effect is smaller than the existing experimental upper bound, which leaves room for reasonably large contributions from the cMSSM. Even more than the previous case, these constraints get tighter as the lower bound is tightened, but often, even with improvements in experimental techniques, this bound remains significantly above the SM prediction, so that there is always some room for a cMSSM contribution. A good example of this is the decay $B_s \rightarrow \mu^+ \mu^-$, where the experimental upper bound on $\text{BR}(B_s \rightarrow \mu^+ \mu^-)$ has been recently improved to 4.5×10^{-9} [6] against a SM prediction of $(3.2 \pm 0.2) \times 10^{-9}$ [15]. In order to take into account the theoretical uncertainties, in our numerical analysis we set the 95% upper limit to be 5.0×10^{-9} . Thus, the cMSSM contribution must satisfy

$$\text{BR}_{\text{cMSSM}}(B_s \rightarrow \mu^+ \mu^-) \leq 1.8 \times 10^{-9} .$$

3. There exists a third – and rare – type of low-energy process where the experimental result is not consistent with the SM prediction at some level between $1-2\sigma$. The experience of the past few decades has generally been that a more accurate measurement of the process, or a more sophisticated computation of the SM prediction generally brings the two into perfect consistency, but there are two results which have till date defied this comfortable precedent. One is the measurement of the anomalous magnetic moment $(g-2)_\mu/2$ of the muon [16,17], and the other is the decay width for $B^+ \rightarrow \tau^+ \nu_\tau$ [18]. In the former case, the SM prediction is too small to explain the experimental data at the level of more than 3σ . For $\mu < 0$,

the cMSSM contributions tend to *decrease* the SM contribution still further, so that the constraints from this process become very strong in this regime. In the case of $B^+ \rightarrow \tau^+ \nu_\tau$, too, the SM prediction is again too low at the level of around 2σ , and once again the cMSSM contributions tend to push the predicted value down rather than up. In fact, if these two anomalies are taken together and at face value, very little of the cMSSM parameter space is still viable [19], and this little bit can barely survive the experimental constraints already available. However, one can argue that if we are to take these discrepancies at face value, then the SM is also ruled out and hence we have already found new physics! In view of the uncertainties in the SM prediction for these processes [20], particularly for $(g-2)_\mu/2$, this is surely too bold a prediction to make at this stage. Hence, if one shrinks from declaring the discovery of new physics in this context, then, by the same token, one must also refrain from declaring the imminent demise of the cMSSM in the same context.

A generic feature of low-energy constraints is that the restrictions obtained from them always assume that the cMSSM (for example) is the only new physics contribution to the relevant process. Obviously, if there are other new physics contributions, the constraints on the cMSSM would change, being either strengthened or relaxed, depending on the relative sign of the two new physics contributions. Of course, one can postulate such effects ad infinitum, and therefore, the usual practice is to invoke Occam's razor and demand that we consider only one sort of new physics at a time. But Nature may well be perverse in this respect, and hence, there is always an element of wishful thinking when we apply any indirect constraints. Ultimately, indirect constraints only become really strong when backed up by direct evidence.

- *Direct searches at high energy colliders:* Like any model of new physics, the cMSSM makes predictions of new particles and interactions, and when one performs a direct search for these in a high energy experiment without observing any of the predicted effects, one ends up ruling out the part of the parameter space.

One of the important features of the cMSSM is that the LSP is always the lightest neutralino $\tilde{\chi}_1^0$ and all SUSY particles undergo cascade decays with the $\tilde{\chi}_1^0$ as the final product. Guaranteed stability by the conservation of R -parity – a crucial feature of the cMSSM – this LSP interacts very weakly with the matter in the detectors and usually flies away to add a minuscule amount to the dark matter component of the Universe, leaving a momentum imbalance in the observed events, which is measured by the missing transverse momentum (MpT) or its equivalent, the missing transverse energy (MET). This missing energy provides a unique way to search for signals of the cMSSM, for any process at a high energy collider which produces a pair of SUSY particles (the pair being required by R -parity conservation) will be followed by direct or cascading decays of these SUSY particles, always ending up in a set of SM particles and large MET.

At the LHC, in particular, the most viable signals will arise when the strongly-interacting SUSY particles, viz. the squarks and the gluinos, are produced in pairs and then each member of the pair decays to other strongly-interacting particles and the LSP, leading to a final state with multiple jets and substantial MET. Searches for such states form the spearhead of the cMSSM effort at the LHC, and also yield the strongest constraints from direct searches. We shall have

more to say on this subject presently.

It is important to note that R -parity conservation is not demanded by any of the underlying symmetries of the cMSSM, and has to be imposed by hand. This may be regarded as another element of wishful thinking in the model. Of course, models with non-conservation of R -parity must violate either lepton number or baryon number and hence, will have their own set of distinctive signals.

- *Dark matter requirements:* Though SUSY was originally invoked to solve the gauge hierarchy-cum-fine tuning problem in the SM, that ‘motivation’ can be argued away if one does not believe in a GUT scale below the Planck scale. However, a more attractive feature of the cMSSM is that the LSP – which is stable and has weak interactions with matter – is just the sort of weakly-interacting massive particle (WIMP) which cosmologists require in order to understand the known behaviour of cosmic dark matter. Here we may recall the two essential features of dark matter. In the first place, it is ‘dark’, i.e. it does not radiate, exactly as a relic density of massive neutralinos might be expected to do. Secondly, it is composed of non-baryonic gravitating matter – probably WIMPs – as is proved rather spectacularly by studies of the Bullet Cluster and similar objects in the Universe.

Purely by studying rotation curves of galaxies and by collecting and collating information about gravitational lensing, one can establish that the amount of dark matter in the Universe is definitely several times more than the amount of visible, baryonic matter. However, the tiny acceleration of the Universe requires a delicate balance between the attractive force of gravitating dark matter and the mysterious repulsive force of dark energy. In fact, to have the working model of inflationary cosmology which will explain the highly-precise Planck data on the cosmic microwave background radiation (CMBR), one requires a rather fine-tuned relic density $\Omega_d h^2$ of dark matter. The specific requirement is that [21]

$$\Omega_d h^2 \simeq 0.1123 \pm 0.0035$$

at 95% C.L. In turn, this imposes constraints on the cMSSM, since all points in the parameter space are not consistent with such a fine-tuned relic density. In the cMSSM, one would require a fine balance between processes which produce neutralino pairs, and co-annihilation processes where a neutralino pair interacts to form ordinary matter.

Apart from the inferences from the dark matter relic density, one can also impose constraints on the parameter space of any model like the cMSSM using the data from direct and indirect searches for dark matter at terrestrial and satellite-based experiments. A comprehensive summary of the results of direct searches can be found in Figure 13 of Ref. [22]. Unfortunately, most of the results from different experiments are, at the moment, not even compatible with each other. It has also been speculated that there may be large uncertainties in the cross-sections of dark matter particles with nucleons [23]. In view of these, we feel that it is premature to use these results to constrain the cMSSM parameter space. Constraints from indirect experiments are rather weak [24], and do not affect our results in any significant way.

It remains, then, to ask how seriously one should take any of the dark matter constraints on the cMSSM. The status of this is really somewhat like the indirect constraints coming from low

energy. For after all, dark matter could be some other form of matter, or even a mixture of neutralinos with some other invisible particles. As before, one can invoke Occam's razor to say that one should consider only single-component dark matter, but in the final reckoning that is mere dogma, and the ultimate test will have to come from a direct discovery. Furthermore, the LSP is stable only if R -parity is conserved, and this, as we have seen, is an ad hoc assumption.

Thus, the cMSSM is constrained in four different ways, each process ruling out some small part of the parameter space, subject to caveats as mentioned above. Taking all factors into consideration, we now make a numerical analysis of the allowed cMSSM parameter space with the following constraints.

1. The ranges of the cMSSM parameters are:

$$0 \leq m_0 \leq 4 \text{ TeV} \quad 0 \leq m_{1/2} \leq 1 \text{ TeV} \quad -1 \text{ TeV} \leq A_0 \leq +1 \text{ TeV} \quad 1 \leq \tan \beta \leq 60$$

with $\mu > 0$, since $\mu < 0$ is strongly disfavoured not only by $(g-2)_\mu/2$ but also by $B \rightarrow X_s \gamma$.

2. For all choices of the parameters the scalar potential must be bounded from below and the LSP must not be the $\tilde{\tau}_1$ (or any other charged particle). These constraints have, of course, been imposed ever since the cMSSM was proposed.
3. The entire set of constraints from the CERN LEP-2 collider data is imposed. The most restrictive among these are the requirements that
 - the mass of the lighter chargino must satisfy $M(\tilde{\chi}_1^\pm) \geq 94.0 \text{ GeV}$ [25], and
 - the mass of the lightest Higgs boson $m_h \geq 93.0 \text{ GeV}$ for $\tan \beta \gtrsim 6$, and $m_h \geq 114.0 \text{ GeV}$ [26] for $\tan \beta \lesssim 6$, with a range of intermediate values in the neighbourhood of $\tan \beta \simeq 6$.

Constraints arising from other considerations (such as, for example, the mass of the lighter stop and the lighter stau) are generally subsumed in the disallowed parameter space due to these two major constraints, but we impose them nevertheless. Like the previous case, these constraints have been in place for some time now, ever since the final data analyses from the LEP Electroweak Working Group became available.

4. The area of parameter space disallowed by direct searches at the LHC is taken over from the ATLAS and CMS Collaborations [4, 5]. These are obtained by combining the negative results of searches in many channels, but the most important of these is the search in the jets + MET channel.
5. Constraints on the cMSSM from the rare decay $B \rightarrow X_s \gamma$ [11] are imposed. The specific requirement is that the cMSSM contribution to the decay width should satisfy

$$-0.55 \times 10^{-4} \leq \text{BR}_{\text{cMSSM}}(B \rightarrow X_s \gamma) \leq 1.35 \times 10^{-4} ,$$

at 95% C.L..

6. Constraints on the cMSSM from the recently-measured upper bound on the rare decay $B_s \rightarrow \mu^+ \mu^-$ [6] are imposed. This measurement has recently been substantially improved by the LHCb

experiment and their updated result has been used in this work. The specific requirement is that the cMSSM contribution to the decay width should satisfy

$$\text{BR}_{\text{cMSSM}}(B_s \rightarrow \mu^+ \mu^-) \leq 1.8 \times 10^{-9} ,$$

at 95% C.L..

7. Finally, we have mapped the part of the cMSSM parameter space which is compatible with the requirement that the observed dark matter component of the Universe be purely a relic density of LSPs $\tilde{\chi}_1^0$. The specific requirement is that

$$0.1053 \leq \Omega_d h^2 \leq 0.1193$$

at 95% C.L. [21] and the stable value of $\Omega_d h^2$ is calculated by solving the relevant Boltzmann equation for the time evolution of the relic density. We do not treat this as a constraint, but merely show the allowed region alongside that permitted by all other considerations.

Apart from the requirement that $\mu > 0$, we have not imposed any specific constraint from the data on $(g - 2)_\mu/2$, and we have chosen not to consider low-energy constraints arising from $B^+ \rightarrow \tau^+ \nu_\tau$. This last has not been taken into account because we feel that the situation vis-a-vis the SM has not yet stabilised and it may be premature to use this to constrain new physics. But all this is not to say that other constraints on the cMSSM parameter space from low-energy data do not exist — in fact, every measurement which is compatible with the SM prediction and has a cMSSM contribution will impose a constraint. However, we find that, except for $(g - 2)_\mu/2$ and $B^+ \rightarrow \tau^+ \nu_\tau$, none of these are as restrictive on the cMSSM parameter space as the set of constraints listed above: the range of parameter space affected by these is always a subset of that ruled out by the combination of those from the above-listed set.

At this juncture, we note that several papers [27] have appeared in which the constraints on the cMSSM from the decays $B \rightarrow X_s \gamma$ and $B_s \rightarrow \mu^+ \mu^-$ have been studied, both independently, and in conjunction with the LHC constraints from direct searches. Some of these have been used to predict the most likely values of the cMSSM parameters. We have chosen the more conservative approach of mapping out the parts of the parameter space which are disallowed, and assuming equal *a priori* probability for the rest. Our presentation of the constraints is, therefore, very close to the way in which direct constraints from the experimental data are available.

We are now in a position to consider the cMSSM parameter space and see how it gets constrained when the above conditions are applied. Our detailed results are given in the next section.

3 Update on the cMSSM Parameter Space

Once we have fixed the sign of μ to be positive, as explained above, the cMSSM parameter space is a four-dimensional space, with the parameters being m_0 , $m_{1/2}$, A_0 and $\tan \beta$, as described above. Since one can plot only two of them at a time, it is traditional to pick two of these parameters and keep the others either fixed, or floating. The most common plots are made in the $m_{1/2}$ - m_0 plane, with A_0

and $\tan\beta$ fixed. This is because the masses of the superparticles depend most directly on these two parameters m_0 and $m_{1/2}$, with the other two contributing mostly through mixing that occurs between pure superparticle states when the electroweak symmetry is broken. For our first plot, therefore, we choose the $m_{1/2}$ – m_0 plane, for three separate values of $A_0 = 0$ and ± 1 TeV, with $\tan\beta = 10$, the last choice being influenced by the latest plots available from the ATLAS and CMS Collaborations. We shall later have occasion to vary A_0 and $\tan\beta$, so this particular choice may be regarded merely as an opening gambit. We generate the cMSSM spectrum using the software SUSPECT [31] and calculate the low-energy observables (including the dark matter relic density) using SUPERISO [32]. Our results are shown in Figure 1. It may be noted that these plots correspond to a top quark mass of 172.9 GeV [25].

The three panels in Figure 1 correspond, from left to right, to choices of $A_0 = +1$ TeV, 0 and -1 TeV respectively. In each panel, we have plotted $m_{1/2}$ in the range 0–1 TeV, and m_0 in the range 0–4 TeV, keeping $\tan\beta = 10$ as mentioned above. It is worth recalling, at this juncture, that the superparticle masses tend to grow with both m_0 and $m_{1/2}$, and hence, may roughly be said to grow along the north-east diagonal of the plot. Thus increased energy of the machine will increase the discovery reach approximately diagonally along these plots, and this is what is, in fact seen.

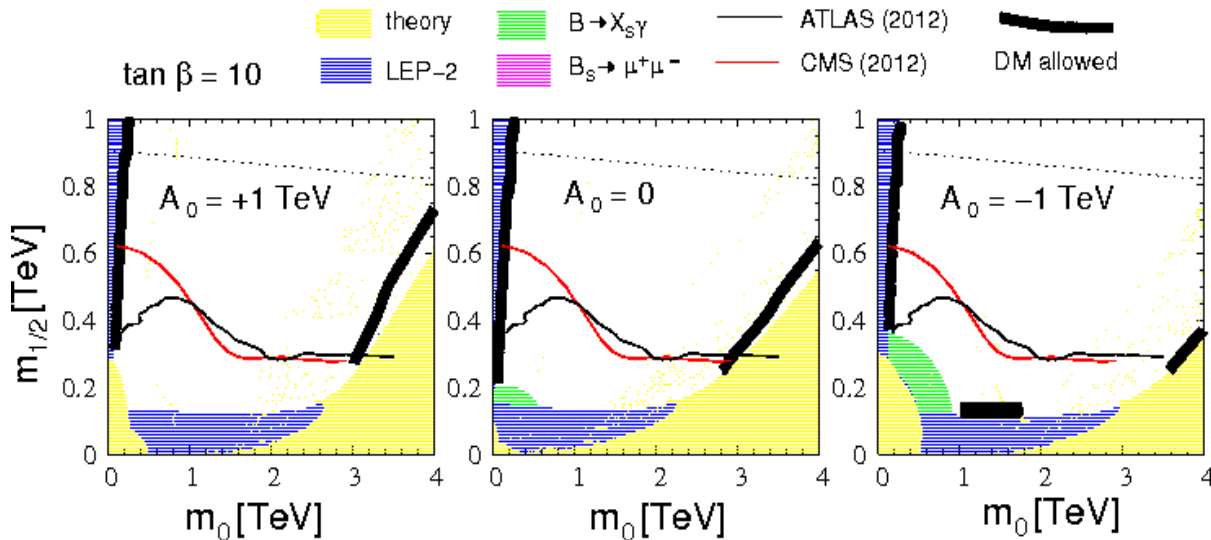


Figure 1: Illustrating constraints on the m_0 – $m_{1/2}$ plane in the cMSSM for $\tan\beta = 10$, as well as the region which explains the observed relic density of dark matter. The details are marked on the different panels or in the key above. The dotted line is the contour for a gluino mass of 2 TeV. Note that $\mu > 0$ for all the plots. The ATLAS and CMS exclusion curves correspond to $A_0 = 0$ but are not very sensitive to A_0 or even $\tan\beta$.

In each plot, the region shaded yellow is ruled out by ‘theory constraints’. Of these, the requirement of vacuum stability is the dominant constraint in the region close to the abscissa and the stau-LSP is the dominant contribution in the region close to the ordinate. For large values of m_0 some of the points are disallowed simply because the renormalisation group equations (RGE) used to calculate the cMSSM spectrum at the electroweak scale have no real solutions. Shapes vary somewhat between the three panels, illustrating the influence of the parameter A_0 on the RGE running of the cMSSM parameters, but the basic features are common, with small values of m_0 and $m_{1/2}$ being ruled out in every case. The regions shaded blue in the three panels of Figure 1 correspond to constraints arising from LEP-2 data. These are generally stronger than the theoretical constraints, except for extreme values of $m_{1/2}$. Most of the LEP-2 disallowed region arises from the chargino mass constraint. The small sliver of space

ruled out by LEP-2 for very low values of m_0 at relatively large values of $m_{1/2}$ corresponds to negative searches for light stau states at LEP-2.

In Figure 1, constraints arising from the non-discovery of cMSSM signals in 4.7 fb^{-1} of data at the ATLAS (CMS) detector are shown by the solid black (red) line, with the region *below* the curve getting ruled out. The ATLAS exclusion curve arises from a combination of all processes, whereas the CMS exclusion plot arises only from searches for the 0 lepton + jets + MET final states made using ‘razor variables’ [5]. These published analyses both choose $A_0 = 0$. Strictly speaking, therefore, this constraint should appear only in the central panel. However, the constraints from a jets + MET search are not very sensitive to the choice of A_0 , and hence, we have made bold to use the same curve for all the three cases. Differences, if any, will be marginal, and should not make any qualitative impact on our discussions regarding these plots. The most important qualitative feature of these constraints is that, unless A_0 is strongly negative, they represent significant improvements over the LEP-2 bounds. As more data is collected and analysed, one may expect the LHC constraints to become stronger, and eventually cover most of the parameter space marked in the panels of Figure 1. It may be noted that though we have not marked any projected reach of the LHC on these plots, a ballpark estimate may be formed from the contour of gluino mass 2 TeV, which is shown by the dotted line near the top of each panel. Therefore, we may conclude that eventually the LHC will be able to explore 80–90% of the parameter space shown in Figure 1, barring the uppermost regions of each panel. Of this, roughly one half is already ruled out, but this is equivalent to saying that roughly one half is still allowed.

The constraints from low-energy data are marked on the graph in green for $B \rightarrow X_s \gamma$ and pink for $B_s \rightarrow \mu^+ \mu^-$. What immediately strikes the eye is the fact that these are rather weak – at least, in the three panels of Figure 1 — where the strongly $\tan \beta$ dependent $B_s \rightarrow \mu^+ \mu^-$ constraint (see below) makes no appearance at all, while the $B \rightarrow X_s \gamma$ data adds on a little to the LEP-2 constraint for $A_0 = -1$ TeV. Even this is totally subsumed in the LHC constraints. One may be tempted to conclude that low-energy measurements are not competitive with the direct searches in constraining the cMSSM parameter space, but we must remember that the plots of Figure 1 are for a fixed value of $\tan \beta$. The situation changes, quite dramatically, when we go to larger values of $\tan \beta$.

Before we go on to discuss high $\tan \beta$ results, however, let us note that the regions in Figure 1 which are consistent with the dark matter (DM) relic density are marked by narrow black bands on all the three plots. This allowed band appears only as the so-called ‘stau co-annihilation region’, i.e. very close to the region disallowed by the stau-LSP constraint, and again for large values of m_0 , in the so-called ‘funnel region’. Nevertheless, it is heartening to see that there is always a region of the parameter space which can be the explanation of the dark matter phenomenon in the cMSSM. This model has not, therefore, lost its most attractive phenomenological feature, and the continuation of at least one small portion of the black bands into the regions inaccessible to the LHC tells us that even if the LHC completes its run without finding any signatures of the cMSSM, we will still be able to argue that the neutralino (albeit a heavier one than we now think) is the main component of the dark matter.

To sum up this part of the discussion, then, *for low values of $\tan \beta$* , for which the value $\tan \beta = 10$ serves as a benchmark, the cMSSM is under no serious threat (unless, as we have seen, constraints from

$(g-2)_\mu/2$ and $B^+ \rightarrow \tau^+ \nu_\tau$ are imposed [19]) from a combination of low-energy data and direct searches. Even if the next round of direct searches throws up a negative result, constraining the parameter space still further, it should not be regarded as the death-knell of the cMSSM, for all that may be happening is that we are in the process of eliminating a barren region in the parameter space as we approach the actual region of interest.

Let us now see what happens when $\tan\beta$ is increased. We have seen that for $\tan\beta = 10$, the only effect of including low-energy constraints is to marginally extend the LEP-2 bound [26], and that too, only for $A_0 = -1$ TeV. This feature continues to hold all the way up to for $\tan\beta = 35$, which covers a substantial fraction of the theoretically allowed range, (viz. up to 60). Around $\tan\beta = 40$, however, the low-energy constraints begin to become significant, and for $\tan\beta = 50$, they outstrip the direct searches and constrain a significant extra part of the parameter space. This is illustrated in Figure 2.

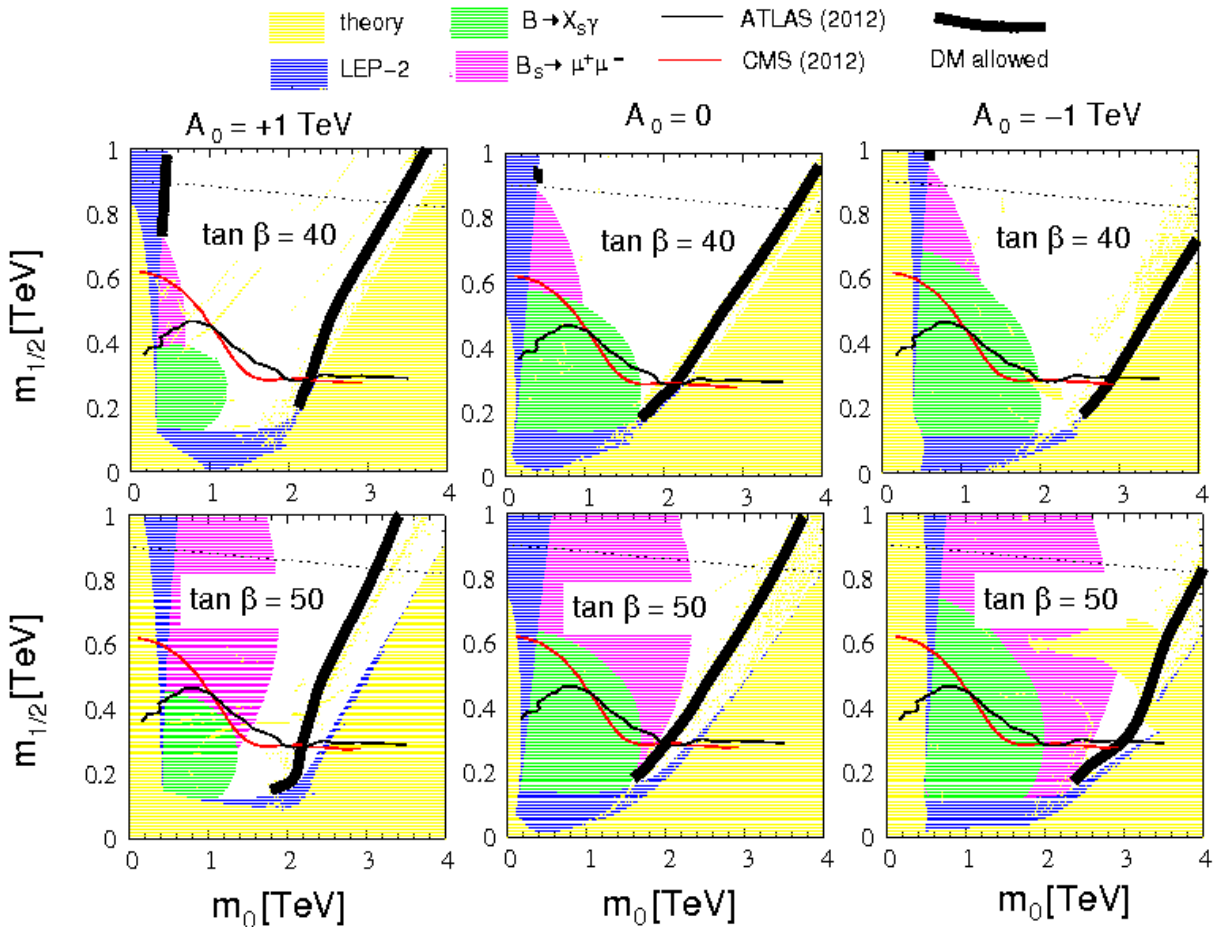


Figure 2: Illustrating constraints on the m_0 - $m_{1/2}$ plane in the cMSSM for high values $\tan\beta = 40, 50$. All notations and conventions are the same as in Figure 1. In these plots B -physics constraints become significant, especially for $A_0 \leq 0$. Note that the dark matter-compatible band always lies in the allowed region. Some of the (yellow) islands indicated as theory-disallowed for large values of m_0 represent numerical instabilities in the spectrum generator SUSPECT.

The conventions followed in Figure 2 are exactly the same as those followed in Figure 1, and are indicated, as in Figure 2, by the little key on the top. The three panels in the first row correspond to $\tan\beta = 40$, while the three panels in the second row correspond to $\tan\beta = 50$. In each row, the three panels correspond to choices of $A_0 = +1$ TeV, 0 and -1 TeV (from left to right). Regions shaded yellow (blue) correspond to constraints from theory (LEP-2), and solid lines marked in black (red)

correspond to the exclusion plot of the ATLAS (CMS) Collaboration². The black strips correspond to regions which are consistent with the neutralino interpretation of dark matter, and the dotted line near the top of each panel corresponds to the contour of $M(\tilde{g}) = 2$ TeV. For large values of m_0 , some of the yellow islands indicating theory-disallowed regions, especially in the bottom right panel, represent numerical instabilities in the spectrum generator SUSPECT, and would be allowed if a different spectrum generator had been used.

Let us begin by discussing the situation for $\tan \beta = 40$, i.e. the upper row of panels in Figure 2. The first thing that strikes the eye is that the theoretically constrained area is larger than in the case of $\tan \beta = 10$, not only in the region which is identified as due to a stau LSP, but over a very large region for higher values of m_0 . The first part is easy to understand, since the off-diagonal terms in the mass matrix for staus $\tilde{\tau}_1, \tilde{\tau}_2$ are proportional to $\tan \beta$. Larger values of $\tan \beta$ can be interpreted as causing a larger splitting between the mass of the heavier and lighter stau, thus pushing the mass of the lighter stau $\tilde{\tau}_1$ downwards, below the mass of the neutralino $\tilde{\chi}_1^0$. This last is not much changed by increasing $\tan \beta$ — a statement which is generically true for all gauginos, including the lighter chargino $\tilde{\chi}_1^\pm$, as a result of which the constrained region from the LEP-2 data remains much the same as before. For large values of m_0 , the RGE evolution is simply not enough to drive one of the scalar mass parameters to negative values, and this manifests as non-convergence of the RGE when we demand such negative values. Alternatively we can simply say that for such parameter choices the electroweak symmetry remains unbroken. Even more than the theoretical constraints, however, for large values of $\tan \beta$ the constraints from low-energy measurements become much more significant. For example, the constraints from $B \rightarrow X_s \gamma$, which made such a modest appearance in the case of $\tan \beta = 10$, now begin to outstrip the LHC exclusion boundaries, especially for $A_0 \leq 0$. Even more dramatic than the growth of the $B \rightarrow X_s \gamma$ constrained region is the appearance of a significant (pink-shaded) region which is now disallowed by the $B_s \rightarrow \mu^+ \mu^-$ constraint. For $\tan \beta = 40$, this is still a smallish appendage to the region already disallowed by other constraints, but if we now look at the lower set of three panels in Figure 2, where $\tan \beta = 50$, it is clear that this new constraint affects large parts of the parameter space which are allowed by all other constraints. This growth in importance of the $B_s \rightarrow \mu^+ \mu^-$ constraint can be readily understood in terms of an enhanced cMSSM contribution from the lighter stop \tilde{t}_1 . As in the case of staus, larger values of $\tan \beta$ increase the diagonal terms in the stop mass matrix and drive the mass eigenvalue corresponding to the \tilde{t}_1 to lower values. Indeed, for large $\tan \beta$, the cMSSM contribution is known [28] to scale as $\tan^6 \beta / (M_{H^+}^2 - M_W^2)^2$.

If we take a quick glance at the lower three panels in Figure 2, one might be tempted to say that a value of $\tan \beta$ as large as 50 seems to be disfavoured because the low-energy constraints combine with the existing ones from theory and direct searches to choke off most of the parameter space accessible to the LHC. However, large $\tan \beta$ values are interesting as they led to distinctive sparticle decay signatures, especially those involving tau final states. It is apparent from the very same figure that the black bands, denoting consistency with the dark matter relic density, go right through the allowed ‘funnel region’ in every panel, showing that a high $\tan \beta$ solution of the dark matter problem is very much a

²We reproduce the exclusion plots already exhibited in Figure 1, which, strictly speaking, are valid only for $\tan \beta = 10$ GeV. However, as we have taken the combined exclusion plot from ATLAS and the purely hadronic exclusion plot from CMS, the larger values of $\tan \beta$ in these plots will not make a significant difference.

viable one.

Given that the m_0 – $m_{1/2}$ plane is so much more constrained, all things taken together, in the high $\tan\beta$ cases, it is natural to ask how accessible the allowed parameter space will be to the LHC runs in the near and more distant future. Of course, once these runs are over, we may expect proper exclusion plots from both ATLAS and CMS Collaborations, but a certain amount of curiosity about what could be the outcome of these runs is inevitable. To satisfy this, we have chosen four benchmark points, within the region mapped in Figure 2, each of which is just allowed by the present constraints and two of which are compatible with the dark matter relic density. The exact choices of parameters corresponding to these points are given in Table 1 below. In the next section we shall take up a more detailed study of cMSSM signals at the LHC for these points.

BP	m_0	$m_{1/2}$	A_0	$\tan\beta$	$\text{sgn } \mu$
A	0.4	0.75	1.0	40.0	+1
B	2.4	0.38	0.0	40.0	+1
C	1.0	0.55	0.0	40.0	+1
D	2.0	0.35	-1.0	40.0	+1

Table 1: The cMSSM parameters for the four benchmark points (BP) chosen for a detailed collider analysis in the context of the current LHC run. The first three columns are in units of TeV. All the points are consistent with the experimental constraints. The points A and B are compatible with neutralino dark matter; C and D are not.

Before taking up detailed collider studies, however, it is instructive to study the cMSSM parameter space in some other ways. For example, since m_0 and $m_{1/2}$ are not the parameters directly measurable at the LHC, one might ask, instead: what are the constraints on the masses of the squarks and gluinos? Here it should be noted that while all the eight gluinos have the same mass $M_{\tilde{g}}$, this is not true of the twelve squarks. This is especially true of the third generation; the squarks of the first two generations are practically degenerate, with $M_{\tilde{q}}$ denoting their common mass.

Figure 3 illustrates the constraints in the upper three panels of Figure 2 (i.e. $\tan\beta = 40$), when translated into the squark-gluino mass plane. Once again, we use the conventions and notations of Figure 1. The most important feature of this graph is the large yellow area ruled out by theory considerations. This arises because the squarks (except in the third generation) are generally heavier than the gluino in scenarios where the lighter stau is heavier than the lightest neutralino. Light gluinos up to a couple of hundred GeV appear to be ruled out by the requirement of vacuum stability. Higher values of the squark mass cannot break the electroweak symmetry unless the gluino is also comparably heavy. There is, then, for all values of A_0 , a funnel-shaped region which is allowed by theoretical considerations. Note that theoretically the gluino can be substantially lighter for $A_0 \leq 0$ than it is for the $A_0 = +1$ TeV case.

As in the previous two figures, we have shown bounds arising from the LEP-2 data by blue shading. As we have seen, this arises principally from the non-observation of chargino pairs, and this bound on the lighter chargino mass translates more-or-less to a constant bound on the gluino mass in the ballpark of 300 – 400 GeV. However, the LHC bounds, shown by solid black (ATLAS) and red (CMS) lines as before, are much stronger, and they push both the squark and the gluino mass to values around a TeV

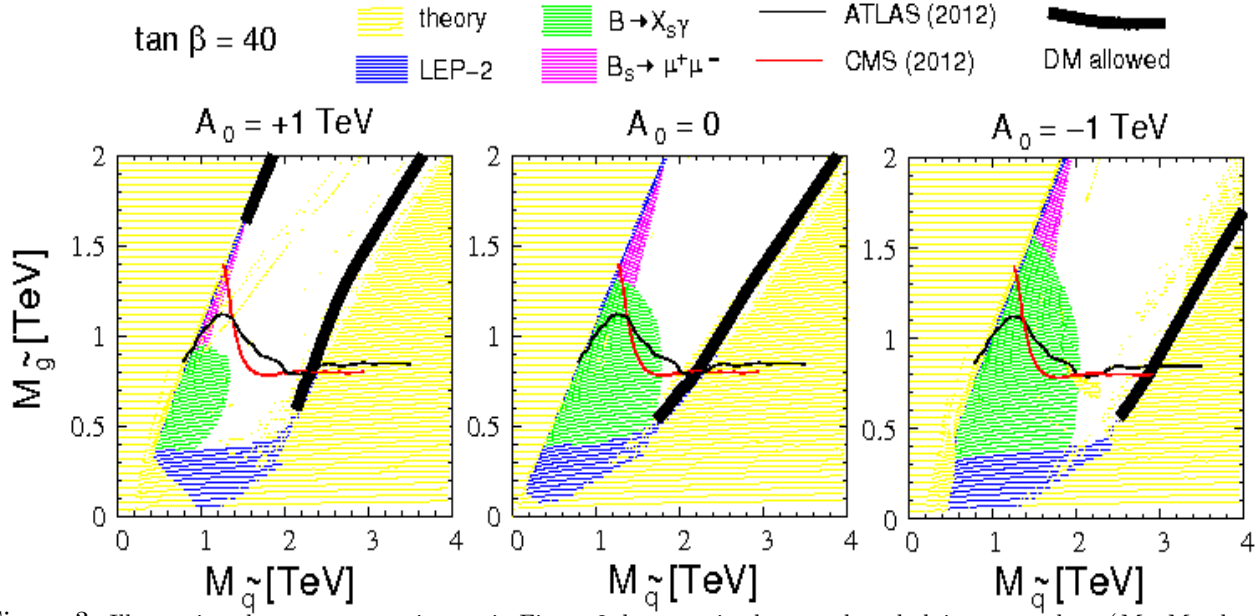


Figure 3: Illustrating the same constraints as in Figure 2, but now in the squark and gluino mass plane ($M_{\tilde{q}}-M_{\tilde{g}}$ plane). All notations and conventions are the same as in Figure 2. However, only the $\tan\beta = 50$ cases are shown.

or more. The effect of the low-energy constraints (the green and pink-shaded regions) is to marginally constrain some of the remaining parameter space. No extra constraint is obtained for $A_0 = +1$ TeV, but modest constraints appear for $A_0 \leq 0$, where the squark mass is pushed up to at least 1.5 TeV. However, if we consider $\tan\beta = 50$ (not shown) most of the allowed region is shut off, and for even higher values of $\tan\beta$, nothing is left of it.

The lesson which is learned from the above studies is that while direct searches for squarks and gluinos at the LHC produce the same kind of constraints for both low and high values of $\tan\beta$ and A_0 , the situation is different for the indirect constraints from low-energy measurements, which are generally stronger as $\tan\beta$ increases and A_0 is driven more strongly negative. To illustrate the full extent of this constraint, in Figure 4, we have plotted the disallowed regions in the plane of $\tan\beta$ and M_A , where M_A is the mass of the physical pseudoscalar A^0 . In this Figure, as in the earlier ones, we show three panels for $A_0 = +1, 0$ and -1 TeV respectively (from left to right) and set $\mu > 0$ throughout. The values of m_0 and $m_{1/2}$ are allowed to range from $0 - 4$ TeV and $0 - 2$ TeV as before. Of course, for a given value of A_0 and $\tan\beta$, these cannot vary independently. In fact, as the variation of M_A is more directly related to that of m_0 , one can imagine $m_{1/2}$ as the floating variable. Thus, if a point in the $\tan\beta-M_A$ plane is marked as disallowed, that means that it is disallowed for *all* values of m_0 and $m_{1/2}$ in the box $m_0 = 0 - 4$ TeV and $m_{1/2} = 0 - 2$ TeV.

In Figure 4, as before, the region shaded yellow indicates that it is ruled out by theoretical considerations, or is not accessible for the given ranges of m_0 and $m_{1/2}$. It is interesting that the disallowed region is very small when $A_0 = 0$, but is significantly larger when $A_0 \neq 0$. This may be traced, as earlier, to a larger mixing among the stau gauge eigenstates, leading to a stau LSP. The LEP-2 constraints do not change much from panel to panel, which is expected, since we have seen that their dependence on m_0 is somewhat weak. What is of greatest interest in Figure 4, however, is the regions ruled out by the low-energy constraints. In each case, it is clear that for $\tan\beta \geq 50$, the constraint

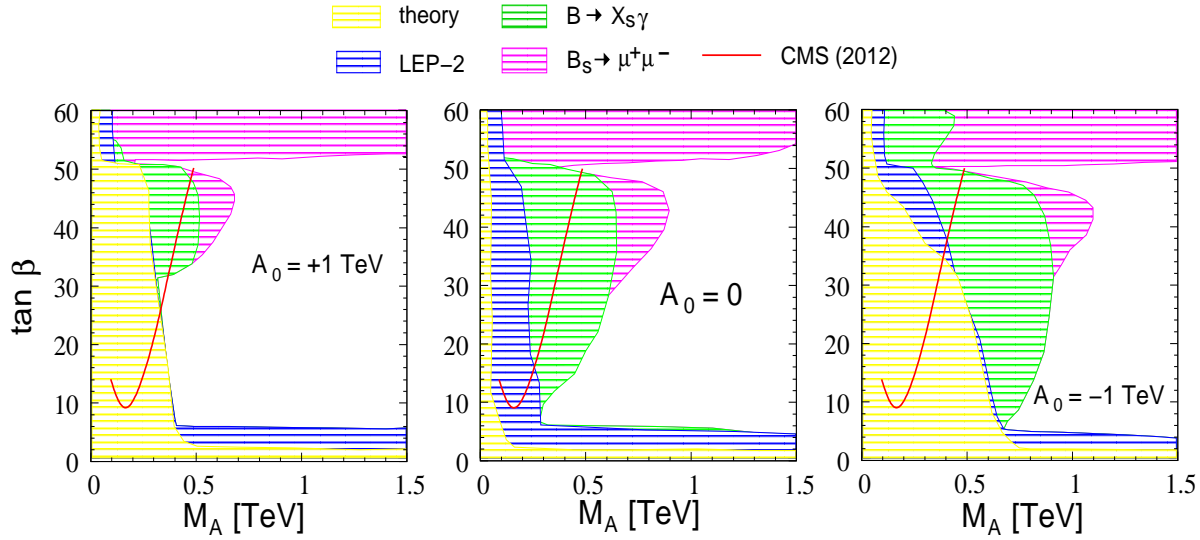


Figure 4: Illustrating the same constraints as before, but now in the $\tan\beta$ – M_A plane. All notations and conventions are the same as in Figure 2, except that m_0 and $m_{1/2}$ are allowed to float in the same ranges as shown in Figure 2. In each panel, regions above and to the left of the red line are disallowed by direct LHC searches by the CMS Collaboration.

from $B_s \rightarrow \mu^+\mu^-$ is highly restrictive, effectively pushing the A^0 mass to the decoupling limit in the Higgs sector. However, this constraint becomes ineffective when the value of $\tan\beta$ is lowered, as we have already seen. In this case, however, the constraint from $B \rightarrow X_s\gamma$ comes into play unless A_0 is large, and this has the effect of driving the mass of M_A to larger values for intermediate values of $\tan\beta$ around 20 – 45. For low values of $\tan\beta$, the low-energy constraints disappear, as we have seen in Figure 1, and we fall back to the LEP-2 constraints. Finally, there is a sort of wedge around $\tan\beta = 50$ where M_A as low as 500 GeV is allowed by all the constraints. Direct searches for the A^0 and the charged Higgs bosons H^\pm at the LHC [29] lead to the exclusion of points above and to the left of the solid red curve — this is, however, less restrictive than the indirect constraints³. If we consider all the diagrams together, we have an absolute minimum of around 300 GeV for the A^0 . This means that the charged Higgs boson, which is easier to detect, is of mass around 310 GeV. In fact, all the heavy scalar states in the cMSSM will now have masses of 300 GeV or above, which already makes them difficult to detect. In this sector, if not in the sector for SUSY particles, the cMSSM is fast approaching the limit where detection at the LHC will no longer be possible.

What about the light scalar state? Obviously, if the heavier scalars start approaching their decoupling limit, the lightest scalar h^0 will also approach its decoupling limit, viz. around 119 – 120 GeV. The exact situation is illustrated in Figure 5, where we plot M_h instead of M_A , keeping m_0 and $m_{1/2}$ floating as before. For this plot, we allow A_0 also to float over all values from –1 TeV to +1 TeV. As before, a point is marked as disallowed if this is valid for all values of m_0 , $m_{1/2}$ and A_0 in the given ranges (only two of these are independent, for reasons explained before).

In Figure 5, as in the others, the region shaded yellow corresponds to the region which is theoretically inaccessible in the cMSSM. Of these, the yellow region on the left of the figure arises because of the

³It is also relevant to note that these constraints were derived in the so-called m_H -max scenario, which is more restrictive than the cMSSM.

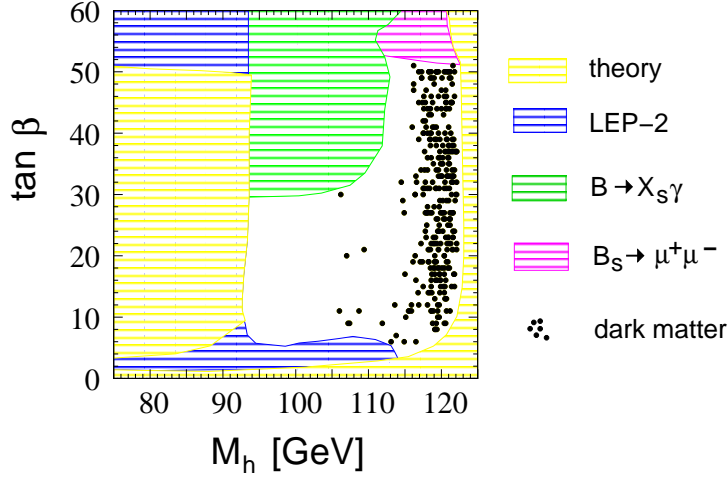


Figure 5: Illustrating the same constraints as before, but now in the $\tan\beta$ - M_h plane. All notations and conventions are the same as before, except that A_0 floats as well as m_0 and $m_{1/2}$. Note that this region is unaffected by the limits from WW^* searches at the LHC.

requirement of vacuum stability and convergence of RGE's, whereas the yellow region on the right is simply not accessible for the parameter range chosen for our study. After all, we must recall that $M_h \leq M_Z$ at the tree-level, and hence much of the region shown in this plot corresponds to radiative corrections to M_h . We shall come back to this issue presently. Of the remaining theoretically-accessible region in Figure 5, a small portion is ruled out by the LEP-2 searches, and comparatively larger regions by the low-energy constraints, especially for large values of $\tan\beta$. However, for $\tan\beta$ in the range 6–30, these constraints allow for M_h anywhere in the region between 93 GeV to about 123 GeV. The lower range in $\tan\beta$ is essentially shut off by a combination of theoretical constraints and LEP-2 bounds.

Much of the above is already well known. The most interesting feature of Figure 5, however, is the cluster of black dots, which indicates the regions compatible with the dark matter requirement. Obviously, these favour a Higgs boson mass in the neighbourhood of 120 – 122 GeV, and strongly disfavour the lighter end of the permitted region. Interestingly, the favoured region is also close to the decoupling regime for the sparticles, and hence, we seem to be looking at a strong hint that the sparticles, if found, will turn out to have masses well in the ballpark of a few TeV.

Recently, the ATLAS and CMS Collaborations, as well as the Fermilab experiments, have reported tantalisingly positive results of their Higgs boson searches, which seem to indicate a Higgs boson of mass somewhere in the region around 125 GeV. The cMSSM prediction, obviously, lies right very close to this. Thus, if this result is confirmed, then, broadly speaking, there will be no problem with the health of the cMSSM. One can even take pride that a light Higgs boson in this regime has been a long-standing prediction of the cMSSM, even in the days when the Higgs boson searches allowed for the entire region from 45 – 800 GeV. However, a closer look at Figure 5 seems to indicate that $M_h = 125$ GeV would be inconsistent with the cMSSM, as we have formulated it, since that value lies in what we have called the theoretically inaccessible region. However, this is not strictly the case, for the upper bound of $M_h \lesssim 123$ GeV which appears from the above plot, is really an artefact of our restricting A_0 to the regime $|A_0| \leq 1$ TeV. Choosing higher values of A_0 can mitigate the upper limit:

for example, if we choose the point

$$m_0 = 4.0 \text{ TeV} \quad m_{1/2} = 1.0 \text{ TeV} \quad A_0 = -6.0 \text{ TeV} \quad \tan \beta = 25 \quad \mu > 0$$

we will predict $M_h \simeq 126 \text{ GeV}$. Obviously, inclusion of a more definite constraint from the light Higgs boson could change our present study quite drastically [30]. For example, if the Higgs boson mass is confirmed to lie around 125 GeV, then the parameter space plotted in all the five figures in this article will become disallowed, and we will only be left with small corners of the parameter space which are compatible with the slightly-larger Higgs boson mass. This study cannot be carried out at the present juncture, because the parameter space is extremely sensitive to the precise value of M_h , with large regions becoming allowed or disallowed for changes in M_h by as little as 1 GeV, whereas the error in the theoretical calculations using SUSPECT is around 2 – 3 GeV. The time for such a study will come when the higher order corrections to M_h are better understood and more precise data are available.

To conclude this section, let us highlight the main results of our analysis of the cMSSM parameter space. The main features are

- The cMSSM is still viable in large parts of the parameter space. This is especially so for $\tan \beta$ in the range from 10 - 35 and $A_0 > 0$, though there are patches which are allowed even outside these ranges. There is no imperative reason, therefore, to write off the cMSSM and invoke one or other of its variants.
- The constraints from low-energy processes such as $B \rightarrow X_s \gamma$ and $B_s \rightarrow \mu^+ \mu^-$ are marginal for large positive A_0 and only become really effective for large negative A_0 and large $\tan \beta$. Other low-energy processes yield even weaker constraints. The two exceptions are the muon anomalous magnetic moment and the rare decay $B^+ \rightarrow \tau^+ \nu_\tau$, which together rule out practically all of the cMSSM parameter space, except a small region which would be accessible to the next set of LHC data analyses.
- Even when all the constraints are imposed, there are enough allowed regions where the cMSSM is compatible with the observed dark matter relic density. This will remain true even if the LHC completes its run without finding signatures of superparticles. However, if the LHC fails to find a light Higgs boson the cMSSM — as indeed the SM and most other supersymmetric models — will be ruled out.
- The heavy scalars of the cMSSM are likely to be too heavy to be seen at the LHC, at least in the early runs. The light scalar should have a mass less than 123 GeV if the SUSY particles are light enough to be seen at the LHC. A light scalar h^0 with mass around 125 GeV is consistent with the cMSSM only in some corners of the parameter space, where the superparticles may well turn out to be too heavy to be seen at the LHC. In this case, the cMSSM will still be a possibility, and will still constitute an explanation for dark matter, but we will have to await a new machine to furnish the experimental proof.

4 Extending the Range of LHC Searches

In the previous section, we have seen that the parameter space of the cMSSM is moderately constrained for large values of $\tan\beta$, but for lower values of $\tan\beta$, the overall constraints are somewhat modest. The strongest constraints arise in this low $\tan\beta$ regime from the direct searches at the LHC. It is important, therefore, to see how far these can explore the parameter space. Of course, with increase in the energy and integrated luminosity, there will always be improvement in the constraints – unless, indeed, we have a discovery – but further extension of the discovery limits will have to depend on our ingenuity in inventing methods to extend the standard searches at the LHC into new regions of parameter space.

In this article we take up one such method which was developed by two of the authors in Ref. [7] to extend the reach of the jets + MET signal which is the major signature of the cMSSM at the LHC. We have earlier mentioned that it is convenient to present our results for four few benchmark points in the parameter space which we have labelled A, B, C and D (see Table 1). All of these are permitted by the combined set of constraints. The first two, viz. A and B, are compatible with neutralino dark matter, while the other two, viz. C and D, are not compatible with dark matter, but are nevertheless, allowed by all terrestrial experiments⁴.

The signals at these four benchmark points (BP) will depend crucially on the mass spectrum at these points. This is readily generated using the package SUSPECT [31], and we present some of the important masses in Table 2 below.

BP	\tilde{g}	\tilde{q}	\tilde{t}_1	\tilde{t}_2	\tilde{b}_1	\tilde{b}_2	\tilde{e}_1	$\tilde{\tau}_1$	$\tilde{\chi}_1^0$	$\tilde{\chi}_2^0$	$\tilde{\chi}_1^+$	$\tilde{\chi}_2^+$	h^0
A	1672	1530	1256	1438	1395	1446	634	596	315	590	590	806	116
B	1018	2480	1533	1860	1860	2113	2400	2031	114	156	156	340	115
C	1307	1512	1080	1292	1267	1353	1080	873	230	436	436	651	116
D	938	2095	1248	1557	1557	1776	2003	1666	148	285	285	530	118

Table 2: Mass spectrum for the benchmark points A, B, C and D given in Table 1. All masses are in units of GeV.

The mass spectrum for the BP's labelled A (DM compatible) and C (DM non-compatible) broadly resemble each other, while those for B (DM compatible) and D (DM non-compatible) are also roughly similar. However, for A the gluino is somewhat heavier than the squarks while in the others it is the squarks which are heavier than the gluinos. The BP labelled A is unique in predicting a light selectron and a light stau which is not surprising, since it has been chosen on the edge of the (excluded) region where we would have a stau LSP. The LSP $\tilde{\chi}_1^0$ varies in mass from the low 114 GeV to the high 315 GeV — both being consistent with $\tilde{\chi}_1^0$ as the principal component of dark matter. For the BP labelled D, the cross-section for producing squarks is clearly negligible and it turns out that electroweak production modes are dominant [33,34]). As all the squarks are heavier than the gluino, the latter will now undergo three-body decays through virtual squarks, but the final states are roughly the same.

⁴Except the muon anomalous magnetic moment and the decay $B^+ \rightarrow \tau^+ \nu_\tau$, which we have not implemented in this work for reasons given in the text.

The production cross-section, for squarks and gluinos at 8 TeV and 13 TeV for these four benchmark points are given in Table 3 below. Both the leading order (LO) and next-to-leading order (NLO) results are calculated using the software PROSPINO [35].

\sqrt{s}	A	B	C	D
8 TeV	1.96 (2.58)	5.45 (15.4)	3.90 (7.21)	11.92 (33.64)
13 TeV	44.9 (59.7)	114.6 (252.6)	97.9 (156.0)	226.8 (486.5)

Table 3: Cross-section at LO in femtobarns for squarks and gluinos at the benchmark points A, B, C and D of Table 1. Numbers in parentheses indicate NLO cross-sections.

A glance at Table 3 tells us that with 10 fb^{-1} of integrated luminosity at the LHC running at a centre-of-mass energy 8 TeV, we may expect to produce anything from a few tens to a few hundreds of squark/gluino pairs through strong interactions, and thus, there is ample scope to detect the signals for these heavy particles decaying through cascades to jets and MET. However, we must recall that all these BP's lie *outside* the published reach of the ATLAS and CMS experiments, which means that these cross-sections are still compatible with the SM background. We shall presently describe a novel set of cuts which can suppress the SM background leaving this signal largely intact, but, for the moment, let us simply note that the cross-sections are at least an order of magnitude larger at 13 TeV, as a result of which these points are very likely to be accessible even to the standard search techniques when the 13 TeV data become available. This is, of course, merely a statement of the obvious, and one could argue that it would be more relevant to look for other BP's where the standard searches at 13 TeV are likely to fail. However, we feel that it would be premature, at this stage, to make predictions for the machine reach at 13 TeV unless we have a better idea of the possible integrated luminosity. For the moment, therefore, we concentrate our efforts on the 8 TeV predictions.

Once produced, the squarks and gluinos will undergo cascade decays of the typical form

$$\begin{aligned} \tilde{g} &\rightarrow q \text{ (jet)} + \tilde{q} \\ &\hookrightarrow q \text{ (jet)} + \tilde{\chi}_1^0 \text{ (MET)} \end{aligned}$$

so that a pair of gluinos will lead to a signal with up to four jets and MET. Of course, this is only one of many possible configurations, given the number and variety of superparticles, but it serves to illustrate the origin and importance of the jets plus MET signal. The dominant SM backgrounds arise from the production of $t\bar{t}$ and W/Z +jets as well as QCD processes — all having cross-sections some orders of magnitude larger than the signal. Eliminating these huge SM backgrounds on the way to isolation of the tiny signal is, therefore, a challenging task, and requires a very finely-tuned set of cuts, which will correspond closely to the signal configurations. We now describe our analysis in some detail, mentioning these cuts as and when relevant.

We have used the well-known Monte Carlo event generator PYTHIA [36] to simulate the signal events as well as backgrounds arising from QCD and $t\bar{t}$ production. Branching ratios for superparticles are calculated using SUSYHIT [37]. For backgrounds arising from W/Z + jets and $t\bar{t}$ + jets we have used ALPGEN [38] interfaced with PYTHIA for showering adopting MLM [39] matching to avoid double counting of jets. We then use FASTJET [40] to obtain jets out of stable particles using the anti- k_T [41]

algorithm with cone size $\Delta R = 0.5$. Jets (J) are selected with a minimum transverse momentum satisfying $p_T^J > 50$ GeV and with pseudorapidity satisfying $|\eta_J| < 3$. We use CTEQ6L as PDF from the LHAPDF package [42]. The missing energy and momentum are estimated, as usual, by summing the energy and momentum of all visible particles.

In addition to these simple acceptance cuts, we apply cuts on the following set of kinematic variables to suppress the large backgrounds in the problem, following earlier work by two of the authors [7].

1. *Transverse events shape variable*: The transverse events shape variable T is defined as,

$$T = \max_{\vec{n}_T} \frac{\sum_J |\vec{q}_T^J \cdot \vec{n}_T|}{\sum_J q_T^J}, \quad (1)$$

where the summation runs over all jets J in the event, \vec{q}_T^J is the transverse component of each jet J and \vec{n}_T is the transverse vector which maximizes this ratio.

As discussed in Ref. [7], for events with low jet multiplicity, such as those belonging to the SM backgrounds, we expect to have $T \sim 1$, whereas for events with high jet multiplicity, such as those belonging to the signal, we expect to have a significant deviation $T < 1$. Therefore, an upper cut on the T variable eliminates a good fraction of the background events without paying much in loss of signal events. In our analysis, we get optimum results by requiring $T \leq 0.9$.

2. *Ratio of sums of jet p_T* : We define the ratio

$$R_T(n_J^{\min}) = \frac{1}{H_T} \sum_{J=1}^{n_J^{\min}} p_T^J \quad (2)$$

where $H_T = \sum_{J=1}^{n_J} p_T^J$, with n_J^{\min} being the lowest number of jets required to trigger the events and n_J being the actual number of jets in the event.

Obviously, events where $n_J \sim n_J^{\min}$ can be expected to yield $R_T \simeq 1$ whereas $n_J \gg n_J^{\min}$ will result in a significant deviation $R_T < 1$ as was observed in Ref. [7]. Hence, as before, a cut on the maximum $R_T(n_J^{\min})$ will suppress the SM backgrounds quite effectively with only a modest loss in signal events. We optimise this as $R_T(4) \leq 0.85$.

3. *Transverse invariant mass between the two leading jets*: We define this as

$$M_T^{12} = \left[2p_T^{J_1} p_T^{J_2} (1 - \cos \phi_{12}) \right]^{1/2} \quad (3)$$

where J_1 and J_2 are the leading (highest p_T^J) jets and ϕ_{12} is the azimuthal angle between them.

This variable is defined primarily to eliminate backgrounds from $t\bar{t}$ events where one would expect the two leading jets to be widely separated, resulting in small values of M_T^{12} . However, in the signal events, the parent particles are comparatively heavier and hence the jets are more evenly distributed. Therefore, demanding larger values of M_T^{12} would remove a sizeable fraction of the $t\bar{t}$ backgrounds with only marginal effects on the signal events. In our numerical analysis, we have set this criterion as $M_T^{12} \geq 450$ GeV.

4. *Missing transverse momentum*: As in all searches for supersymmetry, a cut $\cancel{p}_T \geq 200$ GeV is required to get rid of the remaining background events.

Cut	A	B	C	D	$t\bar{t}$ + jets	QCD	W^\pm + jets	Z^0 + jets	Total SM
Produced	19	55	39	119	1 384 500	3 370 100	6 180 000	1 422 000	22 356 600
$T \leq 0.9$	10	45	30	101	593 978	746 666	2 843 521	768 130	5 952 295
$R_T(4) \leq 0.85$	3	24	17	62	29 928	8 496	1 558	148	110 129
$M_T^{12} \geq 450$ GeV	< 1	13	11	26	907	1263	164	11	32 344
$\cancel{p}_T \geq 200$ GeV	< 1	7	8	13	6	< 1	< 1	< 1	6

Table 4: Cut flow table for the four BP’s A–D and the principal backgrounds. The cross-sections are generated at LO using PROSPINO for $\sqrt{s} = 8$ TeV and the number of events in each entry is for an integrated luminosity of 10 fb^{-1} .

The effect of these cuts on the signal at the four BP’s and on the principal backgrounds is illustrated in Table 4, where we have assumed $\sqrt{s} = 8$ TeV and an integrated luminosity of 10 fb^{-1} . The first row shows the number expected using the LO cross-section using PROSPINO [35] for the signal process. The effect of applying the four special cuts is then apparent from the successive rows. It is obvious that, taken together, these cuts are extremely effective, reducing the SM backgrounds by seven orders of magnitude. In fact, most of the SM backgrounds are removed completely, with the small irreducible portion coming entirely from the $t\bar{t}$ production.

If we consider the numbers presented in Table 4, it is obvious that the cut on T is most effective in suppressing the massive QCD background, while the cuts on $R_T(4)$ and M_T^{12} suppress all the backgrounds, but those from vector boson production more than the others. The final cut on \cancel{p}_T removes all the backgrounds except a small irreducible part from $t\bar{t}$, always the principal bugbear for most new physics studies. However, the combined effect of all the cuts is very impressive, for it reduces a background of a hundred million events to just sixty events, whereas a sizeable fraction of the the few tens of signal events remains.

The last line of Table 4 tells us that it is quite hopeless, at $\sqrt{s} = 8$ TeV, to search for the BP labelled A. In fact, it has been observed [7] that this search technique works better as we go to larger values of m_0 , and we observe that A has the lowest $m_0 = 0.4$ TeV. For the other BP’s, however, if we neglect systematic effects, we should expect to see a signal at a confidence level more than 95% in all cases. Thus, using the present technique, we can hope for (a) either a discovery of the cMSSM in the jets + MET channel during the current year, or at least (b) a significant improvement in the LHC exclusion regions before the machine closes down for the upgrade to 13 TeV. This latter would narrow down the cMSSM search region further, but would not invalidate the cMSSM in any way.

5 Summary

In this article we have critically studied the cMSSM, stressing its strong and weak points, except for its flavour aspects — which call for a different kind of study. In the introductory section we have reiterated that the cMSSM is arguably still the best option where extensions of the SM are concerned, and therefore one should have convincing empirical proof of its demise before other supersymmetric

models can be taken seriously. The cMSSM possesses not just a whole array of pleasing naturalness features, but it also provides an elegant explanation of electroweak symmetry-breaking, which is one of the many artificial contrivances in the SM. The other feature which makes the CMSSM so attractive is that it provides an excellent candidate for a particulate nature of non-baryonic dark matter, which we now know for certain to form a major component of the Universe.

We have then investigated the implications of existing constraints on the cMSSM. These turn out to be of four kinds, viz. (i) *theory constraints* which arise from the cMSSM becoming inconsistent with electroweak symmetry-breaking, (ii) *indirect constraints* which require consistency with low-energy data, especially those coming from B-physics experiments, (iii) *direct constraints* which arise from searches at colliders, of which the LHC searches explore the maximum region of parameter space, and (iv) *dark matter constraints* which arise from the requirement that the observed dark matter is composed of neutralinos. Interestingly, each of the constraints comes with a caveat. The theory constraints affect most those parts of the parameter space where observable signals at colliders are expended; they can be easily evaded at the expense of falsifiability. The indirect constraints arise from virtual superparticle contributions, which can always be mimicked/cancelled by other new physics contributions. Collider searches and a stable neutralino require the conservation of R -parity, which is not demanded by the supersymmetry, but which is put into the cMSSM as a phenomenological nicety. Over and above these, there obviously will be no constraint if there is some other explanation of the dark matter effects.

Despite all these caveats, each of which is equivalent to some level of wishful thinking, we have taken the cMSSM with the whole package of assumptions which go with these caveats, and explored the exact status of its rather limited parameter space when these constraints are applied on it, both individually and in unison. Quite surprisingly, it turns out that the parameter space is only peripherally affected by all these constraints and prejudices. It is only the lower and upper ends of the range in $\tan\beta$ which are absolutely ruled out: the lower end by direct collider searches at LEP-2, and the upper end by a combination of constraints from the low-energy processes $B \rightarrow X_s \gamma$ and $B_s \rightarrow \mu^+ \mu^-$, with the latter making a bigger impact at high values of $\tan\beta$. In the intermediate region, say $\tan\beta \sim 5 - 35$, the only serious constraints come from theory and the direct searches. These leave large areas of the parameter space unexplored, but it is now more-or-less clear that the first two generation squarks and the gluinos of the cMSSM must lie close to or above a TeV in mass. Somewhat higher masses represent no problem for the cMSSM, as a model, but will require more running of the LHC before they can be probed. So far as the superparticle searches are concerned, the results of the early LHC runs can be concisely expressed as (i) a proof that a cMSSM discovery was not ‘around the corner’ when the LHC was turned on, and (ii) that high values of $\tan\beta \gtrsim 50$ are disfavoured.

One of the most interesting features of the constraints on the cMSSM is that so long as some region of the parameter space is permitted, there seems to be a set of points which are compatible with the neutralino explanation of dark matter. In fact, our plots show that even if the LHC completes its run without finding signals for sparticles, there will still exist portions of the parameter space which allow for neutralino dark matter. This is not an issue, therefore, that can be settled by the direct searches.

Perhaps the strongest constraints on the cMSSM will eventually come from the most tenuous of the existing empirical information, viz. the hints for a 125 GeV Higgs boson. For a SM Higgs boson, we have compelling evidence to believe that it cannot lie elsewhere than in the range 115 – 127 GeV. Moreover, there are some excess events over background in several channels for a Higgs boson of mass around 125 GeV. We must remember, however, that the light Higgs boson of the cMSSM is not quite the SM Higgs boson, since there are differences in their couplings to other fields, such as heavy gauge bosons and fermions. Thus the SM Higgs search results cannot be naively taken over into supersymmetry. We have shown that a combination of the existing constraints (and prejudices) indicates a light Higgs boson in the range of around 93 – 123 GeV with the upper part of the range being favoured by dark matter. A light Higgs boson lying in the lower part of this region (say, around 100 GeV), would, therefore, be compatible with all terrestrial experiments, but would require serious re-thinking about the composition of non-baryonic dark matter. On the other hand, a light Higgs boson with mass somewhat higher than 123 GeV would require us to invoke portions of the parameter space which have been left unexplored in the present work, such as very high values of A_0 . Here, every GeV counts – an increase in the light Higgs boson mass by a single GeV would rule out large swaths of the parameter space and vice versa. Thus, it is important to know the exact experimental constraint on the light Higgs boson of the cMSSM which arises from the LHC data. Till such results become available, we can but speculate.

Looking ahead, it seems unlikely that in the near future, low energy constraints from B -physics will improve so dramatically as to make more than incremental changes to the disallowed parameter space as shown in this work. The strongest constraints on the cMSSM parameter space, will, therefore, now come from the LHC direct search data – at 8 TeV, as well as the upgraded run at 13 TeV. It is important, therefore to see just how much of the cMSSM parameter space can be accessed by studying these data. In this context, a search study using event-shape variables has been shown to have a longer reach than other conventional searches. We have, therefore, showcased this by making a detailed study at some chosen benchmark points in the parameter space, which lie in the region allowed by the present data. We show that these could be accessed by our novel study method, and hence, the eventual range of accessible parameter space at the upgraded energy may also be expected to grow accordingly.

All in all, if we consider all the serious empirical evidence available at the present juncture, the cMSSM is still in pretty good health, even though some extremities of the allowed parameter space have been lopped off. However, when more results of the current searches for the Higgs boson become available, it may be tested more stringently than it ever has been in the past. Failure to find a light Higgs boson altogether will certainly spell doom for the cMSSM, as indeed, it will for the SM and the entire picture of electroweak symmetry-breaking which has been built up over the past half-century. A Higgs boson discovery, while vindicating this picture, will be only the start of the real search for supersymmetry, since it will not only make supersymmetry a theoretical necessity, but also provide crucial information on the corner of parameter space in which to search for the superparticles. Anticipating such a discovery, we have explored the potential of a novel background-elimination technique to explore regions in the parameter space where conventional searches cannot penetrate. Whether these will be required or not, however, is a matter which only the future can decide. On this our case rests.

Acknowledgements: DG thanks the Indian Association for Cultivation of Sciences, Kolkata, for hospitality while part of this work was being done.

References

- [1] S. Chatrchyan *et al*, [CMS Collaboration], Phys. Lett. **B710**, 26 (2012), arXiv:1202.1488 [hep-ex].
- [2] G. Aad *et al*, [ATLAS Collaboration], Phys. Lett. **B710**, 49 (2012), arXiv:1202.1408 [hep-ex].
- [3] J. Wess and J. Bagger, *Supersymmetry and Supergravity*, (Princeton University Press, 1991); M. Drees, R.M. Godbole, and P. Roy, *Theory and Phenomenology of Sparticles*, (World Scientific, 2005); H. Baer and X. Tata, *Weak Scale Supersymmetry: From Superfields to Scattering Events*, (CUP, 2006); S.P. Martin, hep-ph/9709356 (1997); E. Cremmer *et al*, Phys. Lett. **B79**, 231 (1978), Nucl. Phys. **B147**, 105 (1979); A.H. Chamseddine, R.L. Arnowitt and P. Nath, Phys. Rev. Lett. **49**, 970 (1982); R. Barbieri, S. Ferrara, and C.A. Savoy, Phys. Lett. **B119**, 343 (1982); L.J. Hall, J.D. Lykken, and S. Weinberg, Phys. Rev. **D 27**, 2359 (1983); P. Nath, R.L. Arnowitt, and A.H. Chamseddine, Nucl. Phys. **B227**, 121 (1983); N. Ohta, Prog. Theor. Phys. **70**, 542 (1983).
- [4] ATLAS Collaboration, Report No ATLAS-CONF-2012-033 (Moriond 2012).
- [5] CMS Collaboration, Physics Analysis Summary, Report No PAS-SUS-12-005 (2012).
- [6] R. Aaij *et al* [LHCb Collaboration], Report No CERN-PH-EP-2012-072, LHCb-PAPER-2012-007 (2012), arXiv:1203.4493 [hep-ex].
- [7] M. Guchait and D. Sengupta, Phys. Rev. **D84**, 055010 (2011), arXiv: 1102.4785[hep-ph].
- [8] See, for example, S.P. Martin in [3].
- [9] H. Baer *et al*, Phys. Rev. **D71**, 095008 (2005); J. Ellis, K.A. Olive and P. Sandick, Phys. Rev. **D78**, 075012 (2008); J. Ellis, K. Enqvist, D.V Nanopoulos and K. Tamvakis, Phys. Lett. **B155**, 381 (1985).
- [10] See, for example, A. Djouadi, arXiv:0503173[hep-ph], and references therein.
- [11] D. Asner *et al*, Heavy Flavor Averaging Group (HFAG) Collaboration, arXiv:1010.1589 [hep-ex].
- [12] M. Misiak, H. M. Asatrian, K. Bieri and M. Czakon *et al*, Phys. Rev. Lett. **98**, 022002 (2007), hep-ph/0609232; M. Misiak and M. Steinhauser, Nucl. Phys. B **764**, 62 (2007), hep-ph/0609241; E. Lunghi and J. Matias, JHEP **0704**, 058 (2007), hep-ph/0612166; A. Freitas and U. Haisch, Phys. Rev. D **77**, 093008 (2008), arXiv:0801.4346 [hep-ph]; S. Descotes-Genon, D. Ghosh, J. Matias and M. Ramon, JHEP **1106**, 099 (2011), arXiv:1104.3342 [hep-ph]; S. Descotes-Genon, D. Ghosh, J. Matias and M. Ramon, PoS EPS **-HEP2011**, 170 (2011), arXiv:1202.2172 [hep-ph].
- [13] J. R. Ellis *et al*, JHEP **0708**, 083 (2007), arXiv:0706.0652 [hep-ph].
- [14] G. Degrandi, P. Gambino and G. F. Giudice, JHEP **0012**, 009 (2000), hep-ph/0009337; P. Gambino and M. Misiak, Nucl. Phys. B **611**, 338 (2001), hep-ph/0104034.

- [15] A. J. Buras, Acta Phys. Polon. B **41**, 2487 (2010), arXiv:1012.1447[hep-ph].
- [16] G. W. Bennett *et al* Muon G-2 Collaboration, Phys. Rev. D **73**, 072003 (2006), hep-ex/0602035.
- [17] M. Davier, A. Hoecker, B. Malaescu and Z. Zhang, Eur. Phys. J. C **71**, 1515 (2011) [Erratum-ibid. C **72**, 1874 (2012)], arXiv:1010.4180 [hep-ph].
- [18] B. Aubert *et al* [BaBar Collaboration], Phys. Rev. D **81**, 051101 (2010), arXiv:0809.4027 [hep-ex]; P. del Amo Sanchez *et al* [BaBar Collaboration], arXiv:1008.0104 [hep-ex]; K. Hara *et al* [Belle Collaboration], Phys. Rev. D **82**, 071101 (2010), arXiv:1006.4201 [hep-ex]; K. Ikado *et al* [Belle Collaboration], Phys. Rev. Lett. **97**, 251802 (2006), hep-ex/0604018.
- [19] B. Bhattacharjee, A. Dighe, D. Ghosh and S. Raychaudhuri, Phys. Rev. D **83**, 094026 (2011), arXiv:1012.1052 [hep-ph].
- [20] E. Lunghi and A. Soni, arXiv:1104.2117 [hep-ph].
- [21] E. Komatsu *et al* [WMAP Collaboration], Astrophys. J. Suppl. **192**, 18 (2011), arXiv:1001.4538 [astro-ph.CO].
- [22] G. Angloher *et al*, Eur. Phys. J. **C72**, 1971 (2012).
- [23] J. Giedt, A.W. Thomas and R.D. Young, Phys. Rev. Lett. **103**, 201802 (2009).
- [24] J. Kersten, talk delivered at WHEPP-XII, Mahabaleshwar, India (January 2012).
- [25] K. Nakamura *et al*, (Particle Data Group), J. Phys. **G 37** 075021 (2010).
- [26] The LEP Working Group for Higgs Boson Searches [ALEPH, DELPHI, L3 and OPAL Collaborations], LHWG-Note-2005-01 (2005).
- [27] S. Akula, D. Feldman, P. Nath, G. Peim., Phys Rev. **D84**, 115011 (2011), arXiv:1107.3535[hep-ph]; C. Beskidt *et al* Phys. Lett. **B705**, 493 (2011), arXiv:1109.6775[hep-ph]; A.G. Akeroyd, F. Mahmoudi and D. Martinez Santos, JHEP **1112**, 088 (2011), arXiv:1108.3018[hep-ph]; O. Buchmueller *et al*, Eur. Phys. J **C72**, 1878 (2012), arXiv:1110.3568[hep-ph]; A. Arbey, M. Battaglia and F. Mahmoudi, Eur. Phys. J. **C72**, 1906 (2012), arXiv:1112.3032[hep-ph]; J.L. Feng, K.T. Matchev and D. Sanford, Phys. Rev. **D85**, 075007 (2012), arXiv:1112.3021[hep-ph]; O. Buchmueller, *et al*, arXiv:1112.3564[hep-ph]; P. Bechtle *et al*, arXiv:1204.4199[hep-ph]; F. Mahmoudi, S. Neshatpour and J. Orloff, arXiv:1205.1845 [hep-ph].
- [28] See, for example, C. Beskidt *et al* in [27].
- [29] S. Chatrchyan *et al*, [CMS Collaboration], CMS-HIG-11-029, CERN-PH-EP-2012-034 (2012), arXiv:1202.4083 [hep-ex].
- [30] H. Baer *et al*, Phys.Rev. **D85** 075010 (2012) arXiv: 1112.3017; A. Arbey *et al*, Phys.Lett. **B708** 162-169 (2012) , arXiv: 1112.3028; S. Akula *et al*, Phys.Rev. **D85** 075001 (2012) , arXiv:1112.3645; J. Cao, Z. Heng, D. Li and J.M. Yang, Phys. Lett. **B710**, 665 (2012), arXiv:1112.4391; J. Ellis and K.A. Olive, arXiv:1202.3262.

- [31] A. Djouadi, J.-L. Kneur and G. Moultaka, Comput. Phys. Commun. **176**, 426 (2007), hep-ph/0211331.
- [32] A. Arbey and F. Mahmoudi, Comput. Phys. Commun. **181**, 1277 (2010), arXiv:0906.0369 [hep-ph].
- [33] H. Baer *et al*, Phys. Rev. **D85**, 055022 (2012), arXiv:1201.2949 [hep-ph].
- [34] D. Ghosh, M. Guchait and D. Sengupta, arXiv:1202.4937 [hep-ph]; P. Byakti and D. Ghosh, arXiv:1204.0415 [hep-ph].
- [35] W. Beenaker, R. Hopker, M. Spira, and P. Zerwas, Nucl. Phys. **B492**, 51 (1997).
- [36] T. Sjostrand, S. Mrenna, P.Z. Skands, J. High Energy Phys. **05**, 026 (2006) , hep-ph/0603175.
- [37] A. Djouadi, M. M. Muhlleitner and M. Spira, Acta Phys. Polon. B **38**, 635 (2007), hep-ph/0609292.
- [38] M.L. Mangano *et al*, JHEP **0307**, 001 (2003).
- [39] S. Hoche *et al*, hep-ph/0602031 (2006).
- [40] M. Cacciari, G.P. Salam and G. Soyez, Eur. Phys. J. **C72**, 1896 (2012), arXiv:1111.6097[hep-ph].
- [41] M. Cacciari, G.P. Salam and G. Soyez, Phys. Lett. **B641**, 57 (2006), hep-ph/0512210.
- [42] H.-L. Lai *et al* [CTEQ Collaboration], Eur. Phys. J. **C12**, 375 (2000).